ELSEVIER

Contents lists available at ScienceDirect

## Journal of Environmental Management

journal homepage: www.elsevier.com/locate/jenvman



## Research article

# Unveiling community adaptations to extreme heat events using mobile phone location data



- <sup>a</sup> Department of Geography, Texas A&M University, College Station, TX 77840, USA
- <sup>b</sup> Department of Atmospheric Science, University of Alabama in Huntsville, AL 35899, USA
- <sup>c</sup> School of Geosciences, University of South Florida, Tampa, FL 33620, USA

## ARTICLE INFO

Keywords: Heatwave Human mobility Adaptation strategies Urban resilience Heat resilience

## ABSTRACT

The escalating frequency, duration, and intensity of extreme heat events have posed a significant threat to human society in recent decades. Understanding the dynamic patterns of human mobility under extreme heat will contribute to accurately assessing the risk of extreme heat exposure. This study leverages an emerging geospatial data source, anonymous cell phone location data, to investigate how people in different communities adapt travel behaviors responding to extreme heat events. Taking the Greater Houston Metropolitan Area as an example, we develop two indices, the Mobility Disruption Index (MDI) and the Activity Time Shift Index (ATSI), to quantify diurnal mobility changes and activity time shift patterns at the city and intra-urban scales. The results reveal that human mobility decreases significantly in the daytime of extreme heat events in Houston while the proportion of activity after 8 p.m. is increased, accompanied with a delay in travel time in the evening. Moreover, these mobility-decreasing and activity-delaying effects exhibited substantial spatial heterogeneity across census block groups. Causality analysis using the Geographical Convergent Cross Mapping (GCCM) model combined with correlation analyses indicates that people in areas with a high proportion of minorities and poverty are less able to adopt heat adaptation strategies to avoid the risk of heat exposure. These findings highlight the fact that besides the physical aspect of environmental justice on heat exposure, the inequity lies in the population's capacity and knowledge to adapt to extreme heat. This research is the first of the kind that quantifies multi-level mobility for extreme heat responses, and sheds light on a new facade to plan and implement heat mitigations and adaptation strategies beyond the traditional approaches.

## 1. Introduction

Over the past decades, there has been an increase in the intensity and frequency of extreme heat events globally, exerting far-reaching impacts on the ecosystems and human health (Tuholske et al., 2021; Zhang et al., 2023). Extreme heat exposure is a serious public health concern, leading to increased morbidity and mortality from a wide range of heat-stress-related diseases (Gasparrini et al., 2015; Deng et al., 2018; Tian et al., 2021; Zhang et al., 2023) and a reduction in labor productivity and economic output (Burke et al., 2015; Day et al., 2019). In the United States, extreme heat is also intensifying. Projections of future climate imply that global temperature will continue to increase through the rest of the century, posing a persistent risk of heat exposure (Diffenbaugh and Moetasim, 2010).

To understand the impacts of heat extremes on human communities,

researchers have developed different assessment frameworks to accurately quantify heat exposure, risk, and impacts (Macintyre et al., 2018; Kovach et al., 2015; Hu et al., 2017). For instance, risk assessment is accomplished by integrally overlaying hazard, exposure, and vulnerability layers. Temperature data is usually used as an input for the hazard layer, socio-economic data for the vulnerability layer, and census data for the exposure layer. A common limitation in existing studies is that the assessment of human heat exposure is primarily based on static census tract-level population survey data. Survey data represent the residential distributions of urban populations, which does not fully capture the daytime population as many urban populations commute for work and schools during weekdays. In addition, census data reflect the multiple average status, for short-term extreme events, the commute-based population mobility is unable to reflect the travel behavior changes (Hu et al., 2017). In a complex urban environment,

E-mail address: hengcai@tamu.edu (H. Cai).

<sup>\*</sup> Corresponding author.

sub-daily dynamic shifts in population distributions can significantly impact individual exposure levels, especially during extreme events (Yang et al., 2019). Some studies highlight that the estimated heat risk and exposure could vary considerably from assumptions based on stationary household settings, and the dynamics of human mobility are not considered (Beckx et al., 2009).

A critical aspect of assessing heat-related exposure effectively is to capture detailed and accurate population distribution. Studies have explored survey-data based human mobility and identified several basic and universal patterns, including periodicity (Liang et al., 2012), high uniformity (Brockmann et al., 2006), and high predictability (Schneider et al., 2013). In recent years, the global spread of mobile devices has enabled the collection of large-scale location data from phone users, which substantially improved the volume, frequency, and representation of human mobility at very fine spatial and temporal scales (Wang et al., 2020). Previous cellular-data-based mobility studies using mobile phone location data revealed that the inherent pattern of mobility was perturbed and usually exhibited significant variations during extreme weather events (e.g., hurricanes, pandemics, and winter storms) (Hatchett et al., 2021; Li et al., 2022; Deng et al., 2021; Xiong et al., 2020; Oiang et al., 2023). For example, Deng et al. (2021) investigated the differences in how different racial and wealth characteristics of population responded to the Hurricane Harvey in the Houston metropolitan area. Xiong et al. (2020) quantified the change of mobility inflows across the United States during COVID-19 and the relationship with infection rates by analyzing location data of over 100 million mobile devices. Li et al. (2022) examined the mobile phone location data of over 90 million individuals in the U.S. during six major disaster events, discovering a consistent hyperbolic decline in human mobility. These variations in mobility patterns can be attributed to several factors, such as reduced capacity of transport infrastructure, poor weather and commuting conditions, disruptions in economic activity and disturbances in social dynamics. How people adapt their movement behaviors in response to extreme heat can be very different from airborne disease transmission, hurricane, and other extreme events. Heat-related human mobility response is often driven more by individual's immediate, spontaneous strategies to cope with the heat, rather than by external factors such as impassable roads and lockdown policy (Carman and Zint, 2020). Furthermore, despite that heat-related deaths and illnesses can be greatly decreased through adaptation measures by reducing extreme heat exposure, the extent to which people employ the behavioral adaptation strategies remain largely unquantified (Fan et al., 2023).

Thermal inequity has drawn growing attention in climate justice and equity. This highlights that, within the context of climate change, some communities or population groups are more vulnerable and face greater heat risks due to differences in socio-economic status, geographic location, or other factors (Zhang et al., 2023; Deng et al., 2020). Research indicates that specific social groups, such as low-income communities and ethnic minorities, tend to be more frequently exposed to high-temperature environments. This increased exposure contributes to a higher risk of health problems within these groups (Yardley et al., 2011). Additionally, individuals residing or working in areas with insufficient green spaces and substandard housing conditions are at an elevated risk of adverse effects from heat waves (Harlan et al., 2006). People's socio-economic backgrounds, combined with environmental factors in their surroundings, lead to diverse coping strategies for extreme heat, particularly in how they move or travel. For example, individuals without air conditioning at home may be more exposed to heat as they travel to places like cooling centers for relief (Widerynski et al., 2017). Thus, using time-sensitive and high-resolution cellular-based location data, we will be able to offer insight not only into the collective adaptation of urban population in a given city but also into intra-urban variations in the response that help to better understand the causes from human perspectives, which are critical to improving the climate justice and environmental equity.

In this study, we leverage anonymized cell phone location data to

analyze human mobility behavior changes in the Houston Metropolitan Area (HMA) during the 2022 heatwave. We developed two indices, the Mobility Disruption Index (MDI) and the Activity Time Shift Index (ATSI), to quantify the differences in human mobility during heatwaves and non-heatwave periods and further examined the relationships between mobility behavior changes and socioeconomic and built environment factors. Three research questions will be addressed: (1) In what ways and to what extent do various urban communities adapt their mobility behaviors in response to extreme heat events in the warmhumid climate region? (2) Do these adaptive mobility behaviors vary spatially and temporally? (3) What are the underlying factors leading to census-block-scale mobility variations?

## 2. Materials and methods

#### 2.1. Study area

We selected the Houston Metropolitan Area (HMA), Texas, USA as the study area. The HMA is located on the Gulf Coastal Plain in southeast Texas and is the fifth-most populous Metropolitan Statistical Area in the United States. HMA spans nine counties and encompasses 3021 census block groups (CBGs), with its division into urban and rural regions (Fig. 1). In 2022, the HMA's population reached 7.34 million, a 1.72% increase from the previous year. This growth rate places it as the second highest among U.S. metropolitan areas (U.S. Census Bureau, 2023). The HMA in humid subtropic climate is well known for its hot, humid summers with temperatures typically between 27 °C and 35 °C from June to August, and mild winters. This climate pattern, along with the HMA's fast urban development and growing population, leads to critical heat-related concerns, including the urban heat island effect, increased population exposure to extreme heat, and adverse health effects (Habeeb et al., 2015; Marsha et al., 2018; O'Lenick Cassandra et al., 2020).

## 2.2. Data collection

## 2.2.1. Mobility data

The mobility data utilized in our study were derived from the ADVAN neighborhood pattern dataset hosted on the DEWEY data platform (https://app.deweydata.io/). This dataset was constructed through algorithmic clustering of pings from over 45 million anonymized mobile devices across the US. Clusters with durations below 1 min were excluded, with each valid cluster labeled as a "visit" and subsequently aggregated by census block group (CBG) to generate the hourly number of visits. It is worth mentioning that the data provider undertook a rigorous examination of potential sampling bias in the foundational panel data by benchmarking it against US Census figures across dimensions like age, race, education, and income. The evaluation affirmed that the sample rate of dataset was approximately 7.5% and provided a representative snapshot of the population (Li et al., 2024). For this specific analysis, to exclude COVID-19-induced human mobility disruptions in 2020, we collected the mobility data for the 3021 census block groups in the HMA for the summers (June-August) of 2019, 2021, and 2022. To ensure comparability across the different years and account for potential variations in the sample size, max-min normalization method was employed to rescale the daily number of visits to a uniform range of [0,1], as shown in Eq. (1):

$$x_{normalized} = \frac{x - min(x)}{max(x) - min(x)}$$
(1)

where x represents the daily number of visits for a given day, while max(x) and min(x) are the minimum and maximum records within the summer period of the respective year.

We extracted the data for the 2022 heatwave period (July 8, 2022 to July 21, 2022, explained in Section 2.3.1) and the corresponding periods

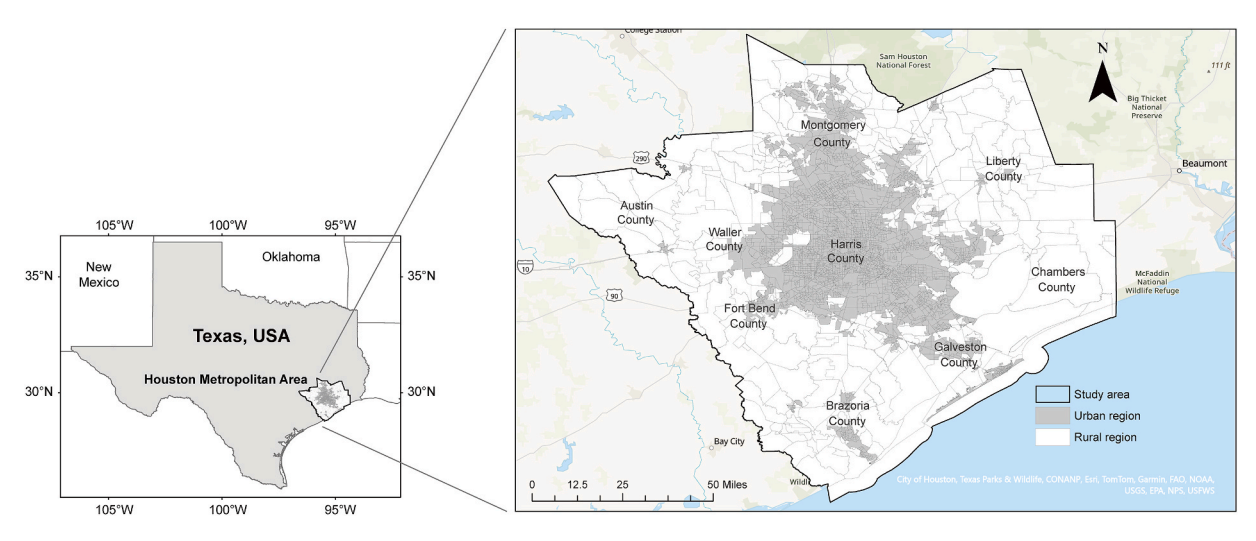


Fig. 1. Study area and boundaries of administrative districts and census block groups, with urban regions shown in gray and rural areas in white.

in 2019 (July 12, 2019 to July 25, 2019) and 2021 (July 9, 2021 to July 22, 2021). This time period selection for 2019 and 2021 was aligned with the day of a week, ensuring that the comparative analysis minimized any potential variances arising from day-specific patterns. In addition, we further expanded the dataset to include data from three weeks before and three weeks after the 2022 heat wave. This additional comparison aims to emphasize the differences in mobility during heatwaves versus non-heatwaves, enhancing the robustness of the results.

#### 2.2.2. Socioeconomic data

Populations' socioeconomic status plays an important role in shaping their behaviors. To account for the relevant factors, we use data from National Historical Geographic Information System (NHGIS) (Manson et al., 2022), based on U.S. censuses and other nationwide surveys. We derived 12 variables from the 5-year American Community Survey database (from 2017 to 2021) within NHGIS. These variables account for the intra-urban mobility variations at the census block group level, including income, population density, ratio of individuals using public transport, and ration of households below poverty level. See Table 1 for detailed information.

#### 2.2.3. Built environment data

To characterize the built environment within census block groups, we derived three factors, including road density, percentage of imperviousness, and percentage of tree cover. Tree canopy cover and imperviousness data for 2021 with a spatial resolution of 30-m were obtained from the Multi-Resolution Land Characteristics (MRLC) Consortium (https://www.mrlc.gov/). These data sets were subsequently aggregated at the census block group level to facilitate the subsequent analyses. The road density was calculated from the road network data obtained from OpenStreetMap (OSP) (https://download.geofabrik.de/), a geographic information platform designed to provide real-time updates and usergenerated content related to its freely available global maps.

We also use the point densities of eight location categories to characterize a community's built environment which play an important role in shaping human movement. The points of interest (POI) data were obtained from SafeGraph Global Places dataset available on the DEWEY data platform. POI data were classified into eight categories: transportation, entertainment, social service, healthcare, restaurant, shopping, manufacturing, and education. The classification is realized by a comprehensive integration of the original POI's attributes. For instance, the POI of social service includes personal and family services, child day care services, nursing services, investigations and security services, and

 Table 1

 Descriptions of each potential driver used in this study.

Category	Variable	Abbreviation	Description
Socio-economic	Income	INCOME	Per capita income for the last 12 months
	Population density	POP_DENS	Population per square kilometer
	Female ratio	FEMALE_RATIO	Percentage of female in the total population
	Elderly ratio	ELDERLY_RATIO	Percentage of people aged 65 and over in the total population
	Minorities ratio	MINORITIES_RATIO	Percentage of people who are minorities in the total population
	Ratio of individuals commuting by car	COMMUTE_BY_CAR	Percentage of workers aged 16 and over who commute by car
	Ratio of individuals using public transport	COMMUTE_BY_PUBLIC	Percentage of workers aged 16 and over who commute by public transport
	Ration of work from home	WFM	Percentage of workers aged 16 and over who work from home
	Ration of with high education	HIGHER_EDUC	Percentage of people with higher education in the total population
	Ration of households without car	WITHOUT_CAR	Percentage of households without a car in total households
	Ration of households below poverty level	POV_RATIO	Proportion of households below the poverty line to total households
Built environment	Road density	RD_DENS	Length of roads per square kilometer
	Percentage of tree cover	TREE_COV	The percentage of canopy cover (30 m)
	Percentage of imperviousness	IMPERV	The percentage of urban impervious surfaces in developed surfaces (30 m)
	Density of transport POI	POI_TRANSP	Number of POI per square kilometer
	Density of social service POI	POI_SOC_SERV	
	Density of restaurant POI	POI_REST	
	Density of manufacturing POI	POI_MANUF	
	Density of healthcare POI	POI_HLTH	
	Density of shop POI	POI SHOP	
	Density of entertainment POI	POI_ENTERTAIN	
	Density of education POI	POI_EDUC	

other services related to buildings and residences. Each category takes its density in its census block groups as a variable.

## 2.3. Methodologies

This study seeks to understand dynamic human mobility behavior changes as an adaptation strategy to extreme heat events, and to identify potential driving factors leading to such changes. Fig. 2 outlines the entire process including three major steps: (1) Developing indices to characterize mobility behavior changes; (2) Collecting and preprocessing the potential drivers; (3) Uncovering potential drivers through causal inference and statistical analysis.

#### 2.3.1. Identification of heatwave

In this case study, daily maximum temperature (May to September) from 1990 to 2022 observed at Houston International Airport from Global Historical Climatology Network daily (GHCNd) database (Menne et al., 2012) is used to identify heatwayes. We defined an episode of heatwave as a period of at least three consecutive days with daily maximum temperatures exceeding the 95th percentile threshold of 32yr summers' daily temperature. In addition, any consecutive days with at least three days exceeding the 95% quantile threshold and the rest period exceeding 90% quantile are also considered as one heatwave episode. In the selected three years, only 1 event was identified as July 8-July 21, 2022 (14 days). For non-heatwave mobility reference, corresponding non-heatwave periods, i.e., July 12 to July 25 in 2019 and July 9 to July 22 in 2021, along with the three weeks preceding and following the 2022 heatwave (June 17, 2022 to July 7, 2022, and July 22, 2022 to August 11, 2022) were used. Recognizing that holiday travel may affect the reliability of the results, we excluded observations on two U.S. public holidays, June 19th and July 4th. We also checked and ensured that there were no synergistic disasters (e.g., floods, hurricanes) that could seriously affect human mobility occurred during all selected periods.

### 2.3.2. Mobility change quantification

We followed the criteria proposed in Zhang et al. (2019), i.e., computable, comparable, and physically meaningful, to design the metric for mobility change. The index requires being derivable from the available human mobility data. The values should allow for benchmarking in different scenarios, and it should be theoretically interpretable with practical relevance. Accordingly, we designed two indices, the mobility disruption index and activity time shift index.

Mobility Disruption Index (MDI): Heatwaves can affect human movement changes to various degrees at any moment of the day. Individuals often adapt to the repercussions of heatwaves by dynamically adjusting their travel preferences and behaviors (Zanni and Ryley, 2015). Consequently, during a heatwave, human mobility fluctuates significantly throughout the entire day compared to normal conditions, which can be quantified by the percentage change in the average mobility value at a specific time during a heatwave, compared to the average mobility value at the equivalent time in non-heatwave conditions, termed as the Percentage Variation in Mobility (PVM). This is mathematically represented as Eq. (2):

$$PVM_t = \frac{\overline{Mob}_{HWt} - \overline{Mob}_{nonHWt}}{\overline{Mob}_{nonHWt}} \bullet 100\%$$
 (2)

where  $\overline{Mob}_{HWt}$  is the average mobility value of a CBG at time t during a heatwave,  $\overline{Mob}_{nonHWt}$  is the average mobility value of the same CBG at the same time t during normal conditions.

The PVM serves as an insightful measure to interpret momentary perturbations in human movement caused by heatwaves. It gauges the relative mobility shifts during any given hour of a heatwave compared to identical hours in non-heatwave situations. To measure cumulative mobility disruptions over time, inspired by Qiang and Xu (2020), we developed the Mobility Disruption Index (MDI) to integrate the intensity and duration of mobility changes, as defined in Eq. (3):

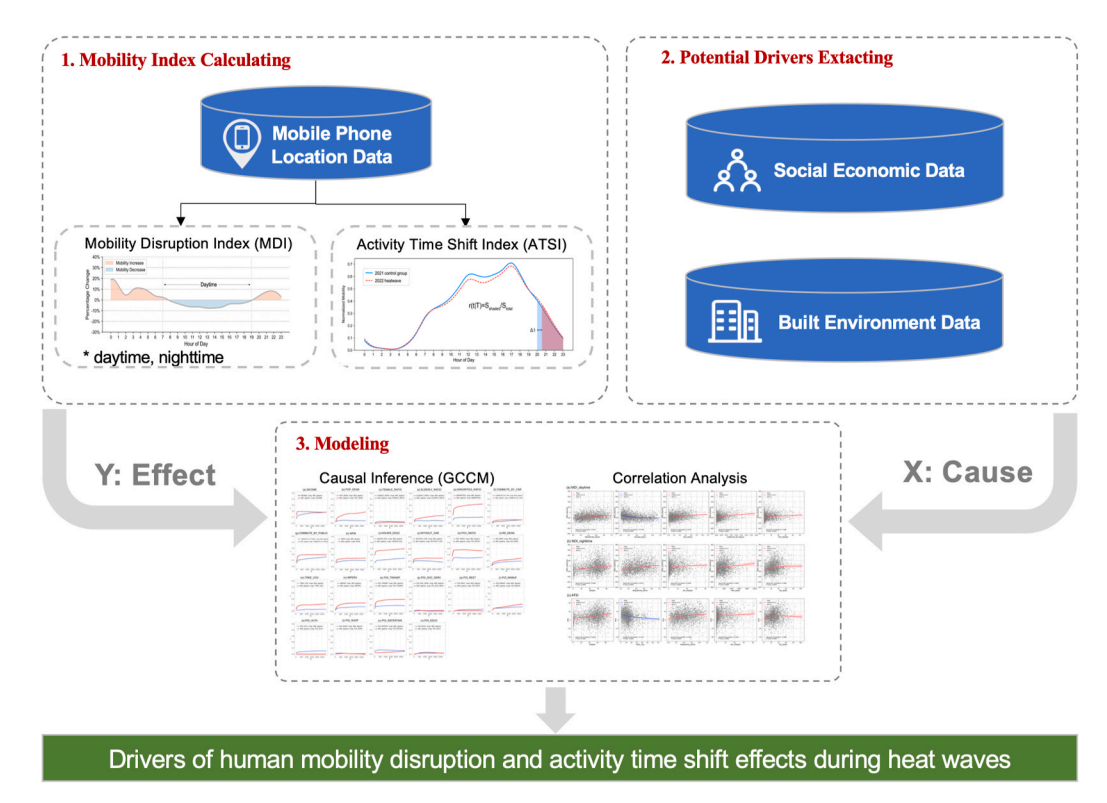


Fig. 2. Flowchart for the assessment of human mobility dynamic changes due to heatwaves. The abbreviations and corresponding descriptions of each potential driver are described in Table 1.

$$MDI = \int_{1}^{t2} PVM_t \tag{3}$$

In this context, MDI represents the net area between the PVM curve and the x-axis over a defined time frame. A positive MDI suggests an increase in mobility during a given time period, while a negative value implies a mobility decrease. The MDI thus captures the cumulative impact of a heatwave event on human mobility dynamics.

Activity time shift index (ATSI): Adjusting or deferring activity schedules is a widely adopted short-term adaptation strategy to reduce extreme heat exposure (Carman and Zint, 2020). To measure the adaptation levels, we developed the Activity Time Shift Index (ATSI) inspired by Fan et al. (2023). The Activity Time Shift Index (ATSI) measures the time adjustment, denoted as  $\Delta h$ , due to heatwave to ensure that the total activity level after a specific hour  $(h + \Delta h)$  is equivalent to the activity after hour h on regular, non-heatwave days. Essentially, it calculates the time shift necessary to align activity levels on heatwave days with those on normal days.

To elaborate, the baseline data is derived from the computed average hourly mobility spanning both heatwave and non-heatwave intervals. The cumulative mobility activity over a designated time frame is calculated through integration. The proportion of human mobility level after a certain time h during a non-heatwave day, r (h | non-heatwaves), is calculated by applying Eq. (4):

$$r\left(h\mid non\_heatwaves\right) = \frac{\int\limits_{h}^{23} Mob_{nonHW}(h)\ dh}{\int\limits_{0}^{2} Mob_{nonHW}(h)\ dh} \tag{4}$$

where  $Mob_{nonHW}(h)$  denotes the average mobility of a CBG at the h hour on a non-heatwave day.

To determine the corresponding mobility level during heatwave days that are equivalent to the mobility level at time h on a non-heatwave day, we calculate the required shift,  $\Delta h$ , from Eq. (5):

$$r(8 p.m. + \Delta h \mid heatwaves) = r(8 p.m. \mid non\_heatwaves)$$
 (5)

We set the activity proportion after 8 p.m. local time during non-heatwave days as the baseline. The time shift  $\Delta h$  ensures that the mobility level after  $(8 + \Delta h)$  *PM* on heatwave days equals the mobility level on baseline days (as depicted in Fig. S1). We chose 8 p.m. as the baseline because it is generally the time of sunset during the summer months in Texas and the secretion of melatonin, which is closely related to human sleep, typically rises during this time (Grivas and Savvidou, 2007). Increased human activity after this time would decrease melatonin production, thus potentially leading to negative effects on sleep.

## 2.3.3. Geographical convergent cross mapping

The relationships between human mobility, climate conditions, and socioeconomic factors are always nonlinear and complex (Xu et al., 2018). Commonly used traditional statistical methods, such as linear correlation analysis, are unable to capture complex nonlinear relationships, thus this research employed an advanced causality analysis method, Geographical Convergent Cross Mapping (GCCM) model (Gao et al., 2023). GCCM is an extension to a cross convergent mapping model that can identify causal associations between spatial cross-sectional variables and estimate the corresponding causal effects. The 23 potential drivers we selected in this study are divided into two categories: socioeconomic variables and built environment variables (Table 1), and the GCCM was utilized to infer their causal relationships with the two indices, MDI and ATSI.

GCCM replaces the lags of time-series observations in traditional cross convergent mapping model with spatial lags (measurements of a

specific unit and its neighbors) to reconstruct a differentiable manifold M in the state space and infer causality based on the cross-mapping (xmap) predictions of the shadow manifolds Mx and My of two spatial variables X and Y. The implementation of GCCM is performed in four steps:

- 1. Reconstruct attractor manifolds of X and Y: With the embedding dimension set to L, the observed values of variables X and Y for each spatial unit at different orders of spatial lag are extracted and organized into vectors,  $\psi(x,s) = [h_s(x),h_{s(1)}(x),...,h_{s(L-1)}(x)]$  and  $\psi(y,s) = [h_s(y),h_{s(1)}(y),...,h_{s(L-1)}(y)]$ . s is the focal unit, s(i) is the i th order of spatial lags, and  $h_{s(i)}(x)$  is the observation function.  $\psi(x,s_1)$ , ...,  $\psi(x,s_i)$  are near neighbors of the focal point  $\psi(x,s)$ , and by combining these vectors one can construct the shaded manifold Mx. My is constructed identically.
- 2. Determination of proximity: When determined  $\psi(x,s)$  is focal point, the states of its near neighbors (e.g.,  $\psi(x,s_1)$ ;  $\psi(x,s_2)$ ;  $\psi(x,s_3)$ ) can be used to identify  $\psi(y,s)$  in the corresponding My manifold. The distance function used for determining the proximity between two states in the shadow manifold is defined in Eq. (6):

$$dis(\psi(x,s_{i}),\psi(x,s)) = \frac{1}{L} \left( \left| h_{s(i)}(x) - h_{s}(x) \right| + \sum_{k=1}^{L-1} abs \left[ h_{si(k)}(x), h_{s(k)}(x) \right] \right)$$
(6)

where abs[\*,\*] is the distance function. If the input data is raster, abs[\*,\*] is defined the averaged absolute difference of each spatial unit; If the input data is polygon, abs[\*,\*] is defined as the absolute difference of spatial lags.

3. Conduct cross-mapping prediction: According to the dynamical systems theory, there is a one-to-one mapping relation between the reconstructed Mx and My. For any given focus state x in Mx, the state y in the corresponding My can be obtained based on the mutual spatial location s and its close states, i.e., cross-mapping prediction, as shown in Eq. (7):

$$\widehat{Y}_{s}|Mx = \sum_{i=1}^{L+1} (w_{si}Y_{si} \mid Mx)$$
(7)

where *s* represents a spatial location in the shadow manifold; *i* is the spatial lag;  $Y_{si}$  is the observation value at the location *s* with the lag of *i*.  $w_{si}$  is the corresponding weight between two states in the shadow manifold;  $\widehat{Y}_s$  is the predicted result.

4. Extract and evaluate causations: The causal associations can be evaluated by the cross-mapping prediction skill  $\rho$ , which is measured by the Pearson correlation coefficient between the observed and predicted values, defined in Eq. (8):

$$\rho = \frac{Cov(Y, \widehat{Y})}{\sqrt{Var(Y)Var(\widehat{Y})}}$$
(8)

where Cov() represents covariance and Var() represents variance. The value of  $\rho$  varies with the size of library (the number of spatial units used to reconstruct the shadow) and the convergence of the GCCM implies that  $\rho$  grows until the library reaches its maximum. The higher the value of convergence  $\rho$  indicates stronger causality. In this process, the embedding dimension starts from L=1 and gradually increases, adding more spatial lags to the state space reconstruction. The optimal L is found when  $\rho$  reaches a plateau, indicating that adding more lags does not significantly improve predictions. The p-value <0.05 indicates that the results are statistically significant, and the confidence interval is 95%.

In this study, we employed the GCCM to explore the causation

between the human mobility indices (i.e., MDI\_daytime, MDI\_nighttime, and ATSI) and each of the potential impact factors. Since the analysis was conducted at the census block group level, the spatial units were census block group polygons. The study area contains a total of 3021 census block groups, which is the size of the library in the GCCM. Based on the arithmetic process described above, we obtained the crossmapping prediction skill  $\rho$  between any mobility change index and potential driver, as well as its variation with the size of the library. Then we plot it for better understanding. For each plot, the x-axis is the size of the library, the y-axis is the value of  $\rho$ , and the line "X xmap Y" denotes the change in  $\rho$  with library growth if Y is set to be the cause and X is set to be the effect. For example, the line "MDI xmap INCOME" is the basis to determine whether INCOME is a cause of MDI (noted as INCOME  $\rightarrow$  MDI). Currently, we may be more focused on the causal strength from potential drivers to human mobility indices.

#### 3. Results

## 3.1. Temporal mobility pattern changes under heatwaves

Fig. 3 illustrates the temporal patterns of human mobility over the entire HMA during the 2022 heatwave compared to the reference periods in 2019 and 2021 and the 2022 non-heatwave. Generally, human mobility shows a consistent daily cyclical pattern during both heatwave and normal conditions. The lowest mobility levels are observed during the late night to early morning hours (0 a.m.–5 a.m.). Subsequently, the mobility gradually increases until it reaches a distinct peak in the midday hours (11 a.m.–2 p.m.). After a brief decline, mobility surges again and peaks throughout the day in the late afternoon to early evening (4 p.m.–6 p.m.). The pattern of mobility on weekdays (Monday to Friday) is relatively stable, whereas the pattern of mobility on weekends (Saturday and Sunday) differs from that on weekdays, especially in the absence of a significant morning peak. This variation is likely attributed to the lack of work/school-related commuting on weekends, granting individuals more flexibility in their outdoor schedules.

Comparing human mobility during the heatwave versus control groups shows that the pattern of population movement during the heatwave in 2022 was significantly different from the other two control groups in 2019 and 2021. For weekdays, there is a significant decrease in mobility during the heatwave, especially at the peak hours in the morning and afternoon. This suggests that individuals potentially adjust or minimize their travel behaviors such as commuting to circumvent peak heat exposures. This trend is further corroborated by weekend data, especially as late afternoon mobility during the heatwave was reduced by about 10-15% compared to non-heatwave periods. Likely, weekends afford people more discretion, hence they opt to remain indoors during heightened temperatures. It is noteworthy that human mobility during the heatwave appeared to increase in part of the night and early morning hours on some days, indicating people's preference to travel during cooler times to escape daytime heat. The comparison of human mobility during the 2022 heatwave with the three-week periods

preceding and following the heatwave further strengthens the robustness of our findings, i.e., the phenomenon of declining mobility during a heatwave.

To understand the differential effects of daytime and nighttime mobility change during heatwave more comprehensively, we defined the period from 7 a.m. to 6:59 p.m. as daytime, and the period from 7 p. m. to 6:59 a.m. the following day as nighttime. We calculated the difference in human mobility at the same moment during heatwave and non-heatwave periods in different years shown in Fig. S2. It is clearly observed that daytime mobility experienced a significant decrease during the heatwave relative to both reference periods in 2019 and 2021. This downturn in mobility is plausibly linked to individuals avoiding exposure to high temperatures during the day. As for nighttime mobility, there is still a discernible decrease, although the decrease in duration and intensity are diminished compared to the daytime. Notably, in comparison to the non-heatwave period of 2021, there are distinct periods during the nighttime when mobility increased significantly. This also demonstrates that people tend to delay their activities to relatively cooler hours.

## 3.2. Travel behavior changes as a heat adaptation strategy

First, the study examined the hourly changes in people's movements (mobility) during the 2022 heatwave and compared it with referenced periods in 2019 and 2021 in the HMA region (Fig. S3). The red dashed line in the graph indicates mobility during the heatwave event, while the green and blue lines represent mobility in the non-heatwave years of 2019 and 2021, respectively. In general, there is a clear decrease in human mobility during the heatwave, especially at rush hours of commuting (e.g., 8 a.m.,12 p.m. and 5 p.m.). Specifically, compared to 2019, mobility during the heatwave begins to significantly decrease earlier in the day, around 5 a.m. (which is about 8 a.m. when compared to 2021). The time when mobility decreases the most within a day also differs against 2019, the largest drop happened around 8 a.m. and 12 p. m., while compared to 2021, it was between 2 p.m. and 3 p.m.

Furthermore, the percentage of hourly mobility changes during a heatwave relative to non-heatwave days was calculated (Fig. 4). Compared to 2019 and 2021, mobility during the 2022 heatwave event exhibited an approximate 10% overall decline at the daytime hours. It is noteworthy that mobility at the nighttime moments under the 2022 heat event shows a significant increase by 10%-20% compared to the same nighttime period in 2021. However, when compared to 2019, there's a noticeable mobility reduction during nighttime relative to the daytime. Based on the percentage change curve of mobility and Eq. (3), the calculated MDI values for daytime and nighttime, compared to the 2019 control group, are -69.78 and -117.07, respectively. When compared to 2021, the MDI values are -52.08 during daytime and 82.25 during the nighttime. For robust check, the daytime MDI is -35.84 and the nighttime MDI is 27.72 when compared to non-heatwave period in 2022. The results all show a significant trend of decreased mobility during the heatwave in daytime.

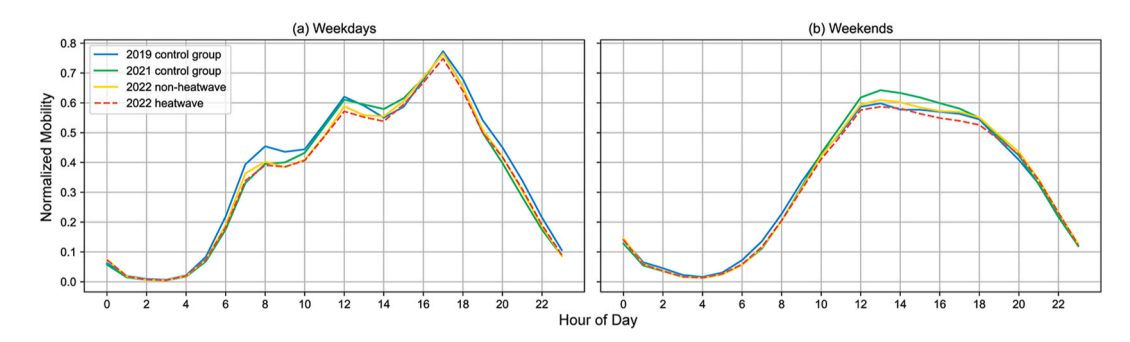


Fig. 3. Mean hour-by-hour changes in human mobility during the 2019 control, 2021 control, 2022 non-heatwave, and 2022 heatwave periods: (a) weekdays; (b) weekends.

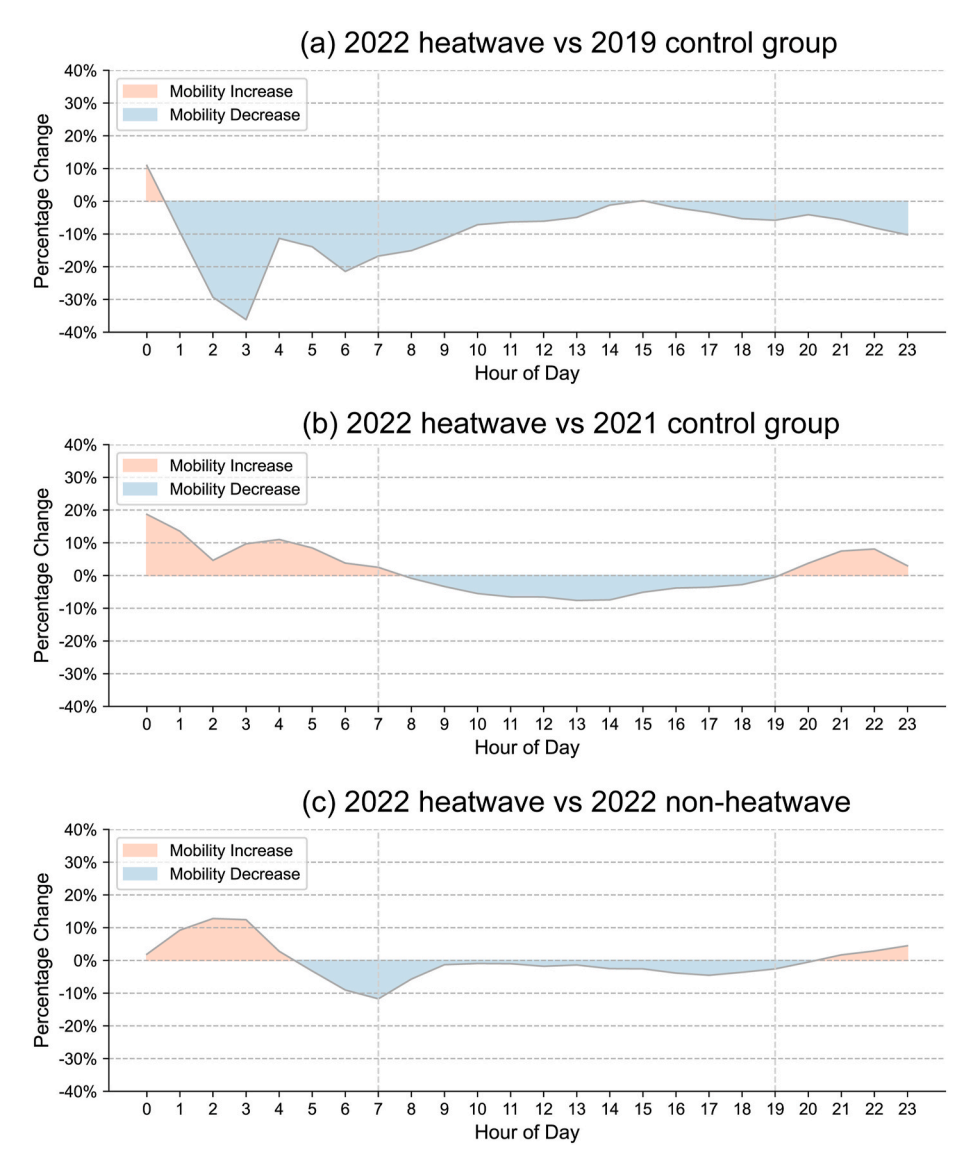


Fig. 4. Hourly percentage change in human mobility during 2022 heatwave compared to (a) 2019 control group, (b) 2021 control group, (c) 2022 non-heatwave.

Fig. 4 suggests that mobility during the 2022 heat wave experienced a notable decrease during both daytime and nighttime when compared to 2019, the pre-Covid-19 control group. This reduction could be attributed to the effects of COVID-19, which had a significant impact on people's behavior, willingness to travel, and travel patterns, as indicated by Abdullah et al. (2020). To isolate the impact of the heat wave and reduce influences caused by COVID-19, we only studied the mobility changes in 2021, the post-Covid 19 non-heat wave period, and 2022, the heat wave event period, for the subsequent analysis.

To further analyze the impact of the heatwave on human mobility in HMA, we examined the spatial disparities Mobility Disruption Index (MDI) during daytime and nighttime at block group level. The results are illustrated in Fig. 5 (a) and (b), in which blue denotes the block groups with negative MDI values, indicating reduced mobility, whereas red block groups with increased mobility with positive MDI values. During the daytime, 88.5% of the total block groups have a negative MDI, indicating that most communities decreased mobility in response to the extreme heat event. A few block groups show an increase in mobility (MDI >0), and these block groups are dispersed without clear clustering. During nighttime, the percentage of block groups with MDI >0 rises significantly from 11.4% during the daytime to about 40%. Notably, in terms of spatial distribution, the block groups with increased mobility are primarily in the central area of the HMA, while those with decreased

mobility are located in the peripheral suburbs.

Fig. S4 compares the Mobility Disruption Index (MDI) values in urban and rural communities during the daytime and nighttime. The average daytime MDIs are similar for both areas (–152.3 for urban and –141.1 for rural), while the average nighttime MDIs rise to 2.7 in urban communities, significantly higher than –75.0 in rural communities. This underscores the different adaptation strategies used by residents in urban versus rural areas during the heatwave event. Additionally, urban communities have better access to air-conditioned entertainment and shopping facilities, helping residents cope with extreme heat. Nevertheless, it is noteworthy that these factors may not be the only drivers of differences in mobility changes between urban and rural communities.

## 3.3. Alteration in the rhythm of nighttime activity

Fig. 5 (c) shows the spatial disparities of the Activity Time Shift Index (ATSI) at block group level. The majority of block groups demonstrated a delay in activity time, thus confirming our hypothesis that people adjust their activity schedules as an adaptation response to extreme heat. Block groups colored green have positive values of ATSI, signifying a delay in the timing of the activity. Conversely, block groups colored red have negative ATSI values, indicating an overall advancement in activity timing during heatwave days. The histogram on the left on Fig. 5

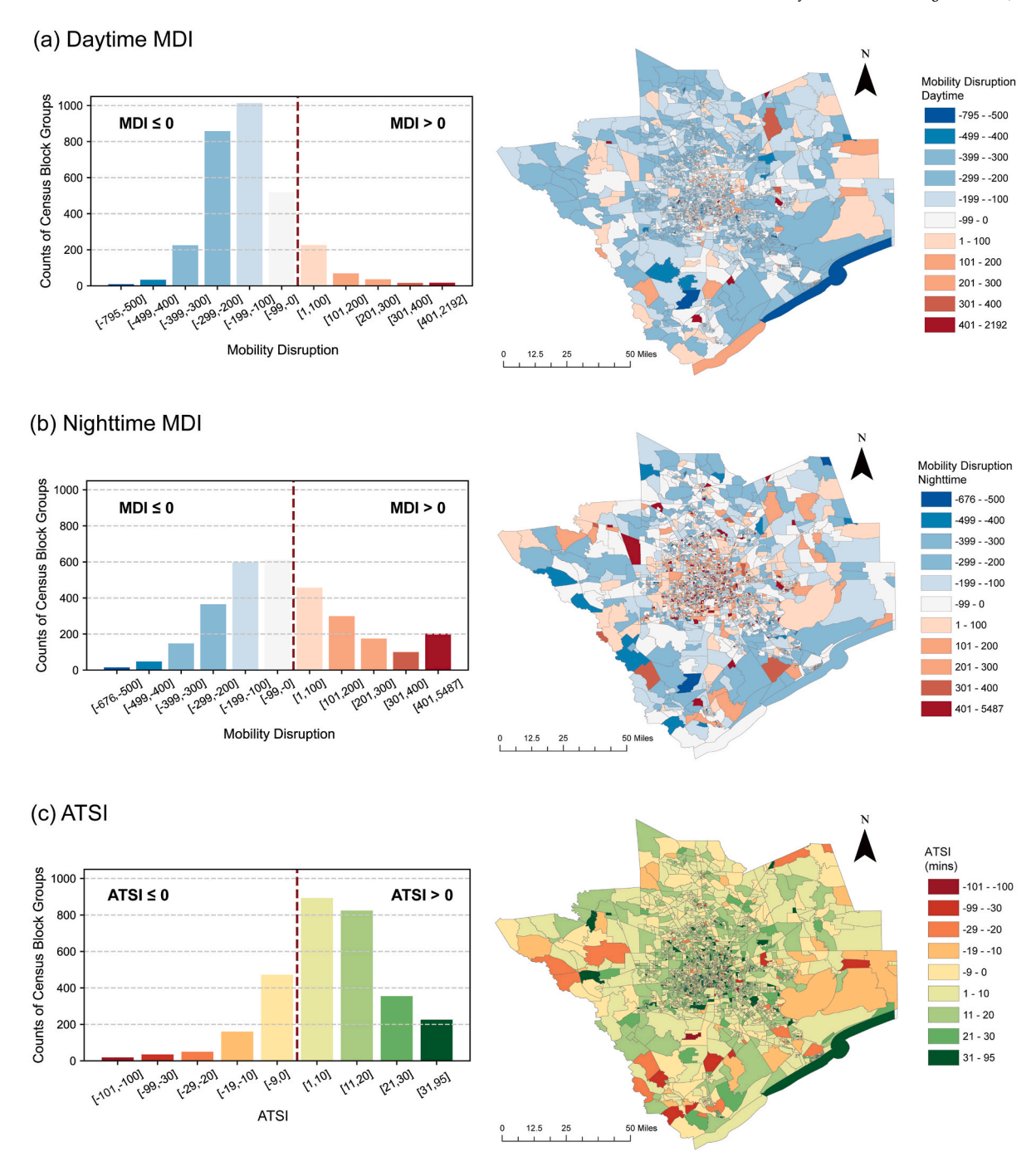


Fig. 5. The spatial distribution of (a) daytime MDI, (b) nighttime MDI, and (c) ATSI, coupled with corresponding counts of census block groups with different levels.

(c) shows that 77.5% of the block groups have ATSI values greater than 0, with an average activity time lag of 17.4 min. Furthermore, the spatial distribution of ATSI shows noteworthy variations, with the central block groups of the HMA displaying a significant delay in activity time, whereas suburban block groups exhibit a less pronounced delay and, in some instances, even an advance in activity time. The comparison of activity time shifts between urban and rural communities (Fig. S5) illustrates that urban communities have an overall ATSI greater than 0, whereas rural communities exhibit significantly lower ATSI values, some even falling below 0. Combined with the findings from the spatial distribution of the MDI (Fig. 5 (a) and (b)), these results reveal that urban communities tend to delay activity to a later time on heatwave days and thus avoid performing outdoor activities during the hottest time during a day. Urban communities experienced exacerbated severity

of heat extremes relative to rural communities, due to the urban heat island phenomena (Jiang et al., 2019). Our result reveals that urban communities are more sensitive and proactive in adapting to heat extremes to mitigate the adverse impacts.

### 3.4. Drivers leading to mobility pattern disparities

In this section, we employed the Geographical Convergent Cross Mapping (GCCM) method for the casual driver detection between the mobility change indices and the potential socioeconomic and built-environment drivers. The nonparametric nature of the GCCM method allows us to investigate causal relationships in complex systems without imposing prior assumptions of linearity or non-linearity. The causal inference results between daytime MDI and the potential socioeconomic

and built-environmental drivers are shown in Fig. 6. Due to page limit, the results for the other two indices, the nighttime MDI and ATSI, are included in Supplemental Figs. S6 and S7, respectively.

In Fig. 6, the red line represents the  $\rho$  (cross-mapping prediction skill) of the daytime MDI xmap potential drivers varying with the size of the L (library), which measures the causal effect intensity of potential drivers on the daytime MDI (noted as potential drivers  $\rightarrow$  daytime MDI, daytime MDI xmap potential drivers). The blue line illustrates the causal impact of daytime MDI on potential drivers. The observed upward trend in  $\rho$  with the expanding library size is justifiable, as larger datasets are utilized in cross-validation during the evaluation of cross-map performance. In this research, we mainly focus on exploring which potential drivers have a strong unidirectional causal effect on the daytime MDI, i. e., the red line exhibits a relatively high cross-mapping ability, and it suffices for another line to maintain a significant gap above it. Notably, the  $\boldsymbol{\rho}$  values of daytime MDI xmap minorities ratio, population density, higher education, poverty ratio and POI of transportation (minorities ratio → daytime MDI, population density → daytime MDI, higher education → daytime MDI, poverty ratio → daytime MDI, and POI of transportation → daytime MDI, respectively) are substantial and statistically significant, as 0.32 (p = 0.00), 0.19 (p = 0.00), 0.30 (p = 0.00), 0.26 (p = 0.00), and 0.19 (p = 0.00). These results underscore the presence of a significant unidirectional causal relationship between these variables and daytime MDI. Conversely, the  $\rho$  values of daytime MDI xmap female ratio, commute by car, and other POI related drivers are much smaller and somewhat nonsignificant, suggesting that these variables have a weaker causal influence or no causation on daytime

MDI. The detailed results of the GCCM tests are summarized in the Supplemental Table S1.

By comparing  $\rho$  values of different potential drivers on the mobility change indices (i.e., daytime MDI, nighttime MDI, and ATSI), we identified the primary drivers leading to mobility change disparities during heatwaves, and the results are shown in Fig. S8. Socioeconomic variables, colored in red in Fig. S8, emerged as the dominant drivers influencing daytime MDI, with minorities ratio, higher education, poverty ratio, commute by public and transportation POI density, ranking among the top five variables in terms of causality. In contrast, nighttime MDI was primarily influenced by the percentage of imperviousness, followed by factors such as the minorities ratio, transportation POI density, population density and road density. Similarly, percentage of imperviousness is also the dominant variable for the ATSI, and subsequently percentage of tree cover, minorities ratio, POI of transportation and road density. Notably, the significant influence of minorities ratio on all mobility change indices underscores a critical issue of climate equity and justice. Furthermore, the percentage with higher education, and poverty ratio significantly influenced the unequal daytime mobility disruptions across communities. This finding highlights the disparities of mobility behaviors across different demographic groups during heatwaves. Built environment factors, including percentage of imperviousness, percentage of tree cover and road density contribute substantially to nighttime MDI and ATSI, which is consistent with our finding that human mobility changes the shifts in activity time vary considerably between urban and rural areas in the nighttime.

One potential driver can either negatively or positively influence

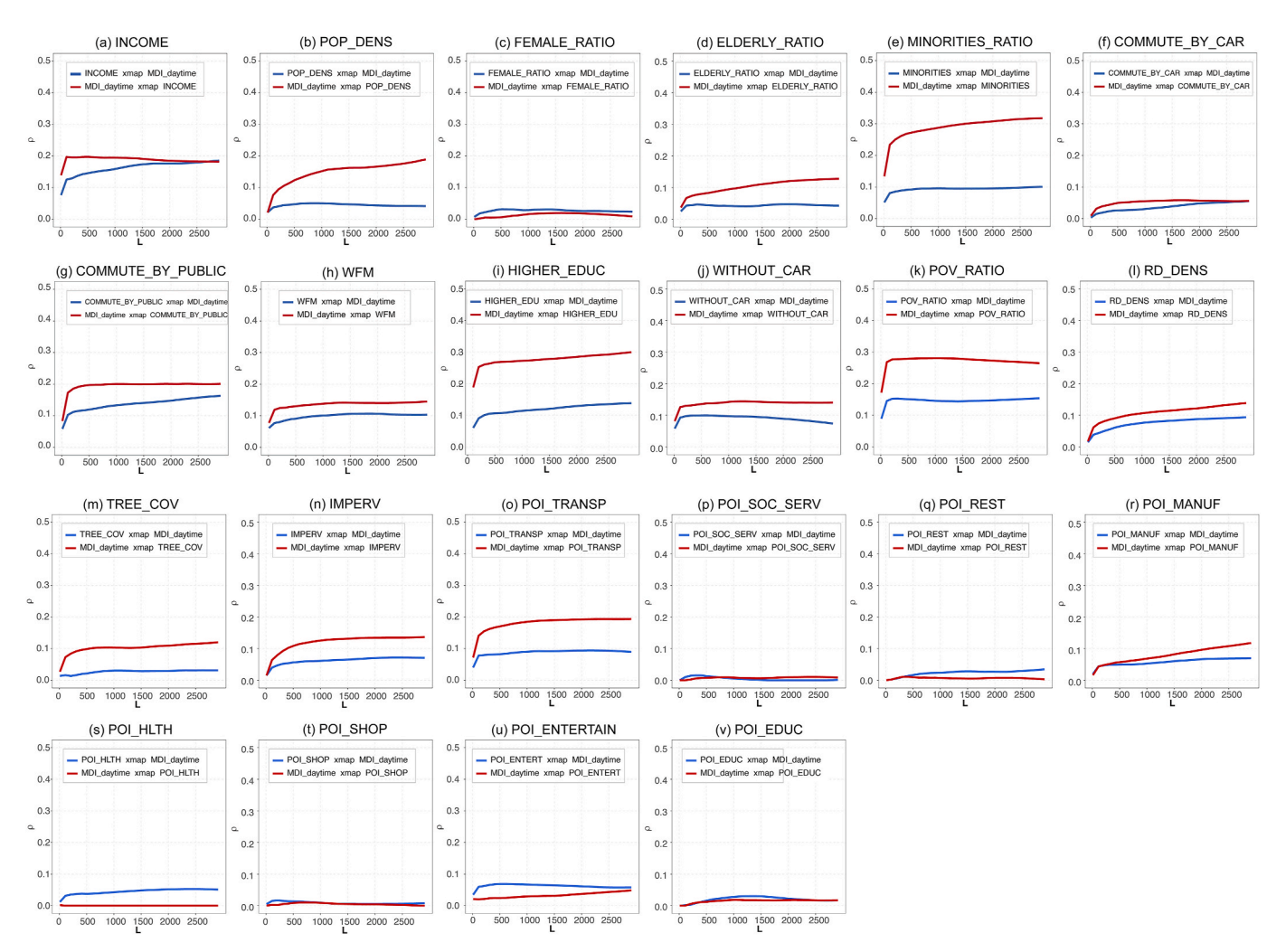


Fig. 6. GCCM causality results for 22 potential drivers and the daytime Mobility Disruption Index (MDI).

mobility behavior changes through different mechanisms (Xu et al., 2018). Given the limitations of the GCCM in determining the direction of causal influences, correlation analysis was then employed as a complementary methodology to further determine the qualitative direction of influence (positive or negative) of the top five ranked potential drivers on the three mobility change indices (Fig. S9). For daytime MDI (Fig. S9. (a)), the minorities ratio and the poverty ratio positively influenced it, indicating that these subgroups of population are less able to reduce their mobility in response to heat extremes, and thus may be subject to greater heat exposure. This finding was consistent with previous studies (Xu et al., 2020; Mitchell and Chakraborty, 2015), suggesting lower socioeconomic and minority status are expected to undertake a higher risk of heat exposure. Results also reveal that factors such as % commute by car and transportation POI density are positively correlated with daytime MDI. Percentage of higher education is negatively correlated with daytime MDI, with a Spearman correlation coefficient of -0.2783(p-value less than  $10^{-4}$ ). Individuals with higher educational attainment often have a better socio-economic standing, providing them the flexibility to plan their schedules and thus avoid traveling during the peak heat hours.

The results also show that all the top five potential drivers ranked by causality strength have a statistically significant positive influence on nighttime MDI (Fig. S9. (b)). The block groups with higher imperviousness ratio as well as higher roads and population density exhibit a less noticeable adaptation response in reduced nighttime mobility during heatwaves. In addition, built environment factors such as imperviousness ratio and road density are statistically significantly positively correlated with ATSI, while tree cover had a Spearman correlation coefficient of -0.1737 (p-value less than  $10^{-4}$ ) with the ATSI, suggesting that the lag in activity time is greater in urban areas than rural areas. Urban regions offer a greater variety of shopping and leisure venues that operate during nighttime, facilitating human activities. In contrast, suburban areas predominantly feature daytime attractions such as parks and scenic spots, resulting in less nighttime activity in these regions. Notably, the minority ratio shows statistically significant positive correlations with both daytime and nighttime MDI and ATSI, suggesting that minority groups are less capable of implementing effective adaptation strategies to reduce mobility during periods of high-temperature heat waves. Consequently, compared to other demographic groups, they bear a greater burden of heat exposure during daytime hours and rely on strategies such as shifting activity time to a cooler time to reduce overall heat exposure. This highlights the need for targeted adaptation strategies to support minority groups in the face of heatwave events.

## 4. Discussion and conclusions

Understanding and accurately quantifying the dynamic patterns of human mobility during extreme heat events is critical to revealing the changes in population exposure under high temperature and to informing policy aimed at minimizing negative health outcomes. Anonymized and privacy-enhanced mobile phone location data provided the timely and fine-scale resources for both local and city-scale response to heat in a humid-hot city. MDI and ATSI indices proposed in the study were proven effectively to capture human mobility perturbations and the time shift of activities using the 2022 heatwave in the HMA as an example. More importantly, these indices are scalable and can be used to analyze human mobility behavior under other hazards such as hurricanes and winter storms. This research not only fills the research gap in existing studies on the assessment of community adaptation strategies under extreme heat events from a human mobility perspective (Carman and Zint, 2020), but also disentangles the potential drivers affecting mobility changes using state-of-art causal inference analysis, which offers insights for heat managements and heat resilience planning and supports the development of actionable measures to mitigate adverse heat impacts.

Existing research has established that human mobility follows

inherent patterns largely based on historical behaviors and frequent visits (Brockmann et al., 2006; Schläpfer et al., 2021). Our study confirms this, finding that human movement is distinctly cyclical and varies between weekdays and weekends. However, extreme events like floods, winter storms, and epidemics can substantially disrupt routine travel behaviors, such as the choice of travel mode, travel time, and travel destinations, thus altering these established mobility patterns (Li et al., 2022). This study discovers that extreme heat events decrease human mobility during daytime hours. Notably, this reduction is not attributable to infrastructure or transportation disruptions from inclement weather (e.g., flooding, earthquake), but rather results from human movement responses to avoid extreme heat exposure during peak temperatures. Concurrently, these adaptation measures lead to behavioral shifts in movement activity, evidenced by heightened nocturnal mobility during heatwaves, suggesting a preference for adjusting movements to a cooler period of the day. Such adaptation responses have significant health implications by reducing exposure to intense heat extremes (Fan et al., 2023).

Additionally, it is important to acknowledge that while the temporal shift in activities as an adaptive response effectively mitigates the adverse impacts of heat exposure, it potentially influences rest-activity cycles. Our research indicates that during heatwaves, most communities in the Houston Metropolitan Area had increased nighttime activities, delaying movement activities for up to 105 min past 8 p.m. Physiological studies have noted that such a delay in nightly activities can chronically disrupt normal circadian rhythms, leading to immediate sleep disturbances and potential psychological consequences (Youngstedt et al., 2019; Pandi-Perumal et al., 2022). These observations underscore the concept of maladaptation and the persisting risks in adapting to climate change (Schipper, 2020). They also highlight the critical importance of considering these behavioral adjustments in future research on heat-related health impacts.

In terms of the analysis of potential drivers of mobility change, to the best of our knowledge, this study is the first to reveal the causation between human mobility and factors like socioeconomic, built environment and POI through causal inference modeling. Previous studies have shown that there is an intertwined and complex relationship between human mobility patterns and socioeconomic indicators (Xu et al., 2018). Therefore, instead of constructing a complex model based on a regression model by combining many possible influencing variables, this case study employed a GCCM that is not constrained by the assumption of linearity or nonlinearity of correlation (Gao et al., 2023). Our causal inference suggested that socioeconomic factors such as the proportion of vulnerable groups (e.g., minorities and poverty) and commuting patterns significantly influence mobility changes during heat waves. This is consistent with previous findings on the relationship between mobility and socioeconomic status, whereby lower socioeconomic populations are more vulnerable to heatwaves, whereas higher-income populations tend to have sufficient capacity to take a variety of adaptive measures to minimize their exposure risks (Xu et al. 2018, 2020; Mitchell and Chakraborty, 2015; Liu et al., 2020). We also observed that built environment factors make an important contribution to mobility changes and delayed activity times at night, and that mobility decreased not significantly in urban areas compared to rural areas during heatwaves. Several studies have inferred that individual heat exposure in urban areas is greater than in rural areas due to factors such as the population structure, cultural differences, and the urban heat island effects (López-Bueno et al., 2022; Hsu et al., 2021; Bernhard et al., 2015). The findings of this study can be supplemented to explain the greater individual heat exposure in urban areas in terms of differences in human adaptive strategies.

Several limitations should be fully acknowledged in this research. First, the mobile phone location dataset is aggregated by census block groups, representing collective behaviors rather than capturing individual-level activities. This aggregation limits the ability to discern specific behavioral adaptations to heatwaves at the personal level.

Furthermore, it is important to recognize that data aggregated to this scale fail to account for intra-block-group movements. Consequently, this would lead to overlooked short-range adaptive behaviors, such as visits to local cooling centers or neighborhood pools located within the same block group. Secondly, the official report states that the dataset has a 7.5% sampling rate of total population (Li et al., 2024). It is inevitable that there are still children, elderly and low-income people who may have been overlooked in this study due to their inability to use mobile devices. Finally, the present study only considered the adaptation behaviors of mobility during heatwaves and did not consider the consequences of possible compound effects such as air pollution and heat. The GCCM has limitations in explaining compounding effects between variables, and further enhancements to the model algorithms need to be explored in the future to improve the explanatory ability. We also not account the urban temperature's spatial variation in mobility analysis. For example, typically stronger nocturnal urban heat islands further influence the urban-rural nighttime mobility differences. Future research could further illustrate those details by focusing on mobility at the point-of-interest level and even at the individual level, incorporating contextual information by combining multisource data (e.g., social media, surveys) to mitigate the bias caused by sample selection. Extreme heat may trigger droughts, wildfires, and air pollution, resulting in compound disaster events that pose a more serious threat to the human community. Therefore, a crucial area of future research is understanding human mobility responses to these complex compound disasters. There are significant differences in the perception of extreme heat by people from different climatic backgrounds, leading to disparities in adaptive behavior, and future research will also focus on comparative analysis of changes in human mobility under extreme heat in multiple cities.

## CRediT authorship contribution statement

Hao Tian: Writing – review & editing, Writing – original draft, Visualization, Methodology, Investigation, Formal analysis, Data curation, Conceptualization. Heng Cai: Writing – review & editing, Writing – original draft, Visualization, Validation, Supervision, Software, Resources, Project administration, Methodology, Investigation, Funding acquisition, Formal analysis, Data curation, Conceptualization. Leiqiu Hu: Writing – review & editing, Methodology, Investigation, Conceptualization. Yi Qiang: Writing – review & editing, Funding acquisition, Conceptualization. Bing Zhou: Writing – review & editing, Methodology. Binbin Lin: Writing – review & editing, Methodology.

## Declaration of competing interest

The authors declare that they have no known competing financial interests or personal relationships that could have appeared to influence the work reported in this paper.

## Data availability

The authors do not have permission to share data.

## Acknowledgements

This article is based on work supported by the U.S. National Science Foundation (Award number: 2117505, 2318204 & 2318206), the National Academies of Sciences, Engineering, Medicine (NASEM) under the Gulf Research Program (Award#: SCON-10000653), and NASA HAQAST (project number: 80NSSC21K0430). Any opinions, findings, and conclusions or recommendations expressed in this material are those of the authors and do not necessarily reflect the views of the funding agencies.

#### Appendix A. Supplementary data

Supplementary data to this article can be found online at https://doi.org/10.1016/j.jenvman.2024.121665.

#### References

- Abdullah, Muhammad, Dias, Charitha, Muley, Deepti, Shahin, Md, 2020. Exploring the impacts of COVID-19 on travel behavior and mode preferences. Transp. Res. Interdiscip. Perspect. 8, 100255 https://doi.org/10.1016/j.trip.2020.100255.
- Beckx, Carolien, Panis, Luc Int, Arentze, Theo, Janssens, Davy, Torfs, Rudi, Broekx, Steven, Wets, Geert, 2009. A dynamic activity-based population modelling approach to evaluate exposure to air pollution: methods and application to a Dutch urban area. Environ. Impact Assess. Rev. 29 (3), 179–185. https://doi.org/10.1016/ i.eiar.2008.10.001.
- Bernhard, Molly C., Kent, Shia T., Sloan, Meagan E., Evans, Mary B., McClure, Leslie A., Gohlke, Julia M., 2015. Measuring personal heat exposure in an urban and rural environment. Environ. Res. 137, 410–418. https://doi.org/10.1016/j. envres.2014.11.002.
- Brockmann, D., Hufnagel, L., Geisel, T., 2006. The scaling laws of human travel. Nature 439 (7075), 462–465. https://doi.org/10.1038/nature04292.
- Burke, Marshall, Solomon, M. Hsiang, Edward, Miguel, 2015. Global non-linear effect of temperature on economic production. Nature 527 (7577), 235–239. https://doi.org/ 10.1038/nature15725.
- Carman, Jennifer P., Zint, Michaela T., 2020. Defining and classifying personal and household climate change adaptation behaviors. Global Environ. Change 61, 102062. https://doi.org/10.1016/j.gloenvcha.2020.102062.
- Day, Ed, Fankhauser, Sam, Kingsmill, Nick, Costa, Hélia, Mavrogianni, Anna, 2019. Upholding labour productivity under climate change: an assessment of adaptation options. Clim. Pol. 19 (3), 367–385. https://doi.org/10.1080/14693062.2018.1517640.
- Deng, Hengfang, Aldrich, Daniel P., Danziger, Michael M., Gao, Jianxi, Phillips, Nolan E., Cornelius, Sean P., Qi, Ryan Wang, 2021. High-resolution human mobility data reveal race and wealth disparities in disaster evacuation patterns. Humanities and Social Sciences Communications 8 (1), 144. https://doi.org/10.1057/s41599-021-00824-8.
- Deng, Hui, Sun, Weizeng, Yip, Wingshan, Zheng, Siqi, 2020. Household income inequality aggravates high-temperature exposure inequality in urban China. J. Environ. Manag. 275. 111224 https://doi.org/10.1016/j.jenyman.2020.111224.
- Deng, Qihong, Zhao, Jinping, Liu, Weiwei, Li, Yuguo, 2018. Heatstroke at home: prediction by thermoregulation modeling. Build. Environ. 137, 147–156. https://doi.org/10.1016/j.buildeny.2018.04.017.
- Diffenbaugh, Noah S., Moetasim, Ashfaq, 2010. Intensification of hot extremes in the United States. Geophys. Res. Lett. 37 (15) https://doi.org/10.1029/2010GL043888.
- Fan, Yichun, Wang, Jianghao, Obradovich, Nick, Zheng, Siqi, 2023. Intraday adaptation to extreme temperatures in outdoor activity. Sci. Rep. 13 (1), 473. https://doi.org/ 10.1038/s41598-022-26928-y.
- Gao, Bingbo, Yang, Jianyu, Chen, Ziyue, George, Sugihara, Li, Manchun, Stein, Alfred, Kwan, Mei-Po, Wang, Jinfeng, 2023. Causal inference from cross-sectional earth system data with geographical convergent cross mapping. Nat. Commun. 14 (1), 5875. https://doi.org/10.1038/s41467-023-41619-6.
- Gasparrini, Antonio, Guo, Yuming, Hashizume, Masahiro, Lavigne, Eric, Zanobetti, Antonella, Schwartz, Joel, Tobias, Aurelio, et al., 2015. Mortality risk attributable to high and low ambient temperature: a multicountry observational study. Lancet 386 (9991), 369–375. https://doi.org/10.1016/S0140-6736(14) 62114-0.
- Grivas, T.B., Savvidou, O.D., 2007. Melatonin the "light of night. In: Human Biology and Adolescent Idiopathic scoliosis." Scoliosis, vol. 2, p. 6. https://doi.org/10.1186/ 1748-7161-2-6
- Habeeb, Dana, Vargo, Jason, Stone, Brian, 2015. Rising heat wave trends in large US cities. Nat. Hazards 76 (3), 1651–1665. https://doi.org/10.1007/s11069-014-1563-z.
- Harlan, Sharon L., Brazel, Anthony J., Prashad, Lela, Stefanov, William L., Larsen, Larissa, 2006. Neighborhood microclimates and vulnerability to heat stress. Soc. Sci. Med. 63 (11), 2847–2863. https://doi.org/10.1016/j. socscimed.2006.07.030.
- Hatchett, Benjamin J., Benmarhnia, Tarik, Guirguis, Kristen, VanderMolen, Kristin, Gershunov, Alexander, Kerwin, Heather, Khlystov, Andrey, Lambrecht, Kathryn M., Samburova, Vera, 2021. Mobility data to aid assessment of human responses to extreme environmental conditions. Lancet Planet. Health 5 (10), e665–e667. https://doi.org/10.1016/S2542-5196(21)00261-8.
- Hsu, Angel, Sheriff, Glenn, Chakraborty, Tirthankar, Diego, Manya, 2021. Disproportionate exposure to urban heat island intensity across major US cities. Nat. Commun. 12 (1), 2721. https://doi.org/10.1038/s41467-021-22799-5.
- Hu, Kejia, Yang, Xuchao, Zhong, Jieming, Fei, Fangrong, Qi, Jiaguo, 2017. Spatially explicit mapping of heat health risk utilizing environmental and socioeconomic data. Environmental Science & Technology 51 (3), 1498–1507. https://doi.org/10.1021/acs.est.6b04355.
- Jiang, Shaojing, Lee, Xuhui, Wang, Jiankai, Wang, Kaicun, 2019. Amplified urban heat islands during heat wave periods. J. Geophys. Res. Atmos. 124 (14), 7797–7812. https://doi.org/10.1029/2018JD030230.
- Kovach, Margaret M., Konrad, Charles E., Fuhrmann, Christopher M., 2015. Area-level risk factors for heat-related illness in rural and urban locations across North

- Carolina, USA. Appl. Geogr. 60, 175–183. https://doi.org/10.1016/j.apgeog.2015.03.012.
- Li, Weiyu, Qi, Wang, Liu, Yuanyuan, Small, Mario L., Gao, Jianxi, 2022. A spatiotemporal decay model of human mobility when facing large-scale crises. Proc. Natl. Acad. Sci. USA 119 (33), e2203042119. https://doi.org/10.1073/pnas.2203042119
- Li, Zhenlong, Ning, Huan, Jing, Fengrui, Lessani, M. Naser, 2024. Understanding the bias of mobile location data across spatial scales and over time: a comprehensive analysis of SafeGraph data in the United States. PLoS One 19 (1), e0294430. https://doi.org/ 10.1371/journal.pone.0294430.
- Liang, Xiao, Zheng, Xudong, Lv, Weifeng, Zhu, Tongyu, Xu, Ke, 2012. The scaling of human mobility by taxis is exponential. Phys. Stat. Mech. Appl. 391 (5), 2135–2144. https://doi.org/10.1016/j.physa.2011.11.035.
- Liu, Sida, Chan, Emily Yang Ying, Goggins, William Bernard, Huang, Zhe, 2020. The mortality risk and socioeconomic vulnerability associated with high and low temperature in Hong Kong. Int. J. Environ. Res. Publ. Health 17 (19), 7326. https:// doi.org/10.3390/ijerph17197326.
- López-Bueno, J.A., Navas-Martín, M.A., Díaz, J., Mirón, I.J., Luna, M.Y., Sánchez-Martínez, G., Culqui, D., Linares, C., 2022. Analysis of vulnerability to heat in rural and urban areas in Spain: what factors explain Heat's geographic behavior? Environ. Res. 207, 112213 https://doi.org/10.1016/j.envres.2021.112213.
- Macintyre, H.L., Heaviside, C., Taylor, J., Picetti, R., Symonds, P., Cai, X.M., Vardoulakis, S., 2018. Assessing urban population vulnerability and environmental risks across an urban area during heatwaves implications for health protection. Sci. Total Environ. 610–611, 678–690. https://doi.org/10.1016/j.scitotenv.2017.08.062.
- Manson, Steven, Schroeder, Jonathan, Van Riper, David, Kugler, Tracy, Ruggles, Steven, 2022. IPUMS national historical geographic information system: version 17.0. In: Minneapolis. MN. IPUMS.
- Marsha, A., Sain, S.R., Heaton, M.J., Monaghan, A.J., Wilhelmi, O.V., 2018. Influences of climatic and population changes on heat-related mortality in Houston, Texas, USA. Climatic Change 146 (3), 471–485. https://doi.org/10.1007/s10584-016-1775-1.
- Menne, Matthew J., Durre, Imke, Vose, Russell S., Gleason, Byron E., Houston, Tamara G., 2012. An overview of the global historical climatology network-daily database. J. Atmos. Ocean. Technol. 29 (7), 897–910. https://doi.org/10.1175/JTECH-D-11-00103.1.
- Mitchell, Bruce C., Chakraborty, Jayajit, 2015. Landscapes of thermal inequity: disproportionate exposure to urban heat in the three largest US cities. Environ. Res. Lett. 10 (11), 115005 https://doi.org/10.1088/1748-9326/10/11/115005.
- O'Lenick Cassandra, R., Baniassadi, Amir, Michael, Ryan, Monaghan, Andrew, Boehnert, Jennifer, Xiao, Yu, Hayden Mary, H., et al., 2020. A case-crossover analysis of indoor heat exposure on mortality and hospitalizations among the elderly in Houston, Texas. Environmental Health Perspectives 128 (12), 127007. https://doi.org/10.1289/EHP6340.
- Pandi-Perumal, Seithikurippu R., Cardinali, Daniel P., Zaki, Nevin F.W., Karthikeyan, Ramanujam, Spence, David Warren, Reiter, Russel J., Brown, Gregory M., 2022. Timing is everything: circadian rhythms and their role in the control of sleep. Front. Neuroendocrinol. 66, 100978 https://doi.org/10.1016/j. vfrne.2022.100978.
- Qiang, Y., Xu, J., 2020. Empirical assessment of road network resilience in natural hazards using crowdsourced traffic data. Int. J. Geogr. Inf. Sci. 34 (12), 2434–2450. https://doi.org/10.1080/13658816.2019.1694681.
- Qiang, Yi, Zou, Lei, Cai, Heng, 2023. Big Earth Data for quantitative measurement of community resilience: current challenges, progresses and future directions. Big Earth Data 1–23. https://doi.org/10.1080/20964471.2023.2273594.
- Schipper, E. Lisa F., 2020. Maladaptation: when adaptation to climate change goes very wrong. One Earth 3 (4), 409–414. https://doi.org/10.1016/j.oneear.2020.09.014. Schläpfer, Markus, Dong, Lei, O'Keeffe, Kevin, Santi, Paolo, Szell, Michael,
- Salat, Hadrien, Anklesaria, Samuel, Vazifeh, Mohammad, Ratti, Carlo,

- West, Geoffrey B., 2021. The universal visitation law of human mobility. Nature 593 (7860), 522–527. https://doi.org/10.1038/s41586-021-03480-9.
- Schneider, Christian M., Belik, Vitaly, Couronné, Thomas, Smoreda, Zbigniew, González, Marta C., 2013. Unravelling daily human mobility motifs. J. R. Soc. Interface 10 (84), 20130246. https://doi.org/10.1098/rsif.2013.0246.
- Tian, Hao, Zhou, Yumin, Wang, Zihui, Huang, Xiaoliang, Ge, Erjia, Wu, Sijia, Wang, Peng, Tong, Xuelin, Ran, Pixin, Luo, Ming, 2021. Effects of high-frequency temperature variabilities on the morbidity of chronic obstructive pulmonary disease: evidence in 21 cities of Guangdong, South China. Environ. Res. 201, 111544 https://doi.org/10.1016/j.envres.2021.111544.
- Tuholske, Cascade, Kelly, Caylor, Funk, Chris, Verdin, Andrew, Sweeney, Stuart, Grace, Kathryn, Peterson, Pete, Evans, Tom, 2021. Global urban population exposure to extreme heat. Proc. Natl. Acad. Sci. USA 118 (41), e2024792118. https://doi.org/10.1073/pnas.2024792118.
- U.S. Census Bureau, 2023. Large southern cities lead nation in population growth. https://www.census.gov/newsroom/press-releases/2023/subcounty-metro-micro-estimates.html. (Accessed 27 August 2023).
- Wang, Yanxin, Li, Jian, Zhao, Xi, Feng, Gengzhong, Luo, Xin, 2020. Using mobile phone data for emergency management: a systematic literature review. Inf. Syst. Front 22 (6), 1539–1559. https://doi.org/10.1007/s10796-020-10057-w.
- Widerynski, Stasia, Schramm, Paul J., Conlon, Kathryn C., Noe, Rebecca S., Grossman, Elena, Hawkins, Michelle, Nayak, Seema U., Roach, Matthew, Hilts, Asante Shipp, 2017. Use of Cooling Centers to Prevent Heat-Related Illness: Summary of Evidence and Strategies for Implementation.
- Xiong, Chenfeng, Hu, Songhua, Yang, Mofeng, Luo, Weiyu, Zhang, Lei, 2020. Mobile device data reveal the dynamics in a positive relationship between human mobility and COVID-19 infections. Proc. Natl. Acad. Sci. USA 117 (44), 27087–27089. https://doi.org/10.1073/pnas.2010836117.
- Xu, Rongbin, Qi, Zhao, Coelho, Micheline S.Z. S., Saldiva, Paulo H.N., Abramson, Michael J., Li, Shanshan, Guo, Yuming, 2020. Socioeconomic level and associations between heat exposure and all-cause and cause-specific hospitalization in 1,814 Brazilian cities: a nationwide case-crossover study. PLoS Med. 17 (10), e1003369 https://doi.org/10.1371/journal.pmed.1003369.
- Xu, Yang, Belyi, Alexander, Bojic, Iva, Ratti, Carlo, 2018. Human mobility and socioeconomic status: analysis of Singapore and Boston. Comput. Environ. Urban Syst. 72, 51–67. https://doi.org/10.1016/j.compenvurbsys.2018.04.001.
- Yang, Jiachuan, Hu, Leiqiu, Wang, Chenghao, 2019. Population dynamics modify urban residents' exposure to extreme temperatures across the United States. Sci. Adv. 5 (12), eaav3452 https://doi.org/10.1126/sciadv.aav3452.
- Yardley, Jane, Sigal, Ronald J., Kenny, Glen P., 2011. Heat health planning: the importance of social and community factors. Global Environ. Change 21 (2), 670–679. https://doi.org/10.1016/j.gloenvcha.2010.11.010.
- Youngstedt, Shawn D., Elliott, Jeffrey A., Kripke, Daniel F., 2019. Human circadian phase–response curves for exercise. J. Physiol. 597 (8), 2253–2268. https://doi.org/ 10.1113/JP276943.
- Zanni, Alberto M., Ryley, Tim J., 2015. The impact of extreme weather conditions on long distance travel behaviour. Transport. Res. Pol. Pract. 77, 305–319. https://doi. org/10.1016/j.tra.2015.04.025.
- Zhang, Fucheng, Li, Zaishang, Li, Nan, Fang, Dongping, 2019. Assessment of urban human mobility perturbation under extreme weather events: a case study in Nanjing, China. Sustain. Cities Soc. 50, 101671 https://doi.org/10.1016/j.scs.2019.101671.
- Zhang, Hui, Luo, Ming, Pei, Tao, Liu, Xiaoping, Wang, Lin, Zhang, Wei, Lin, Lijie, Ge, Erjia, Liu, Zhen, Liao, Weilin, 2023. Unequal urban heat burdens impede climate justice and equity goals. Innovation 4 (5). https://doi.org/10.1016/j. xinn.2023.100488.
- Zhang, Xin, Chen, Fanglin, Chen, Zhongfei, 2023. Heatwave and mental health.
  J. Environ. Manag. 332, 117385 https://doi.org/10.1016/j.jenvman.2023.117385.